

Hierarchical Nanostructures of Fluorinated and Naked Ta₂O₅ Single Crystalline Nanorods: Hydrothermal Preparation, Formation Mechanism and Photocatalytic Activity for H₂ Production

Junyuan Duan,^a Weidong Shi,^a Leilei Xu, Guangying Mou, Quanliang Xin and Jianguo Guan*

State Key Laboratory of Advanced Technology for Material Synthesis and Processing, Wuhan University of Technology, Luoshi Road 122#, Wuhan 430070, P. R. China.

^a These 2 authors contributed equally to this work.

* Corresponding Author, Tel: 86-27-87218832, Fax: 86-27-87879468 ,
E-mail: guanjq@whut.edu.cn

Experimental Section

Chemicals: Hydrofluoric acid (HF, 99.6%, AR, 40 wt %), hydrogen peroxide (H₂O₂, 99.9%, AR, 30 wt %), methanol (99.9%, AR) and metallic tantalum powders (99.5% purity) and commercial Ta₂O₅ particles (C-Ta₂O₅) were purchased from commercial suppliers and used without further purification. Deionized water (10 MΩ·cm) was used in the all reactions.

Synthesis of F-Ta₂O₅ HNs: In a typical synthesis procedure, 25 mg tantalum powders (black-color), 12.5 mL of 0.133 M hydrofluoric acid (HF) aqueous solution, and 4.0 mL of 30 wt % hydrogen peroxide (H₂O₂) solution were mixed and then transferred into a Teflon-lined autoclave with a volume of 25 mL, which was subsequently heated at 240 °C for 12 h in a box furnace. (Caution! Hydrofluoric acid is highly corrosive and it must be handled carefully.) After the autoclave was cooled to room temperature naturally, the final white-color precipitates were separated, washed with ethanol for three times and then dried in oven at 60 °C for 6 h to obtain the final products of F-Ta₂O₅ HNs.

Synthesis of Ta₂O₅ HNs: the typical F-Ta₂O₅ HNs were calcinated in a tube furnace at 700 °C for 3 h with a heating rate of 5 °C min⁻¹ in air, then cooled down to room temperature naturally.

Characterization: The phase analyses of the samples were performed by X-ray diffraction (XRD; Rigaku, D/MAX-RB), using Cu K α radiation ($\lambda=1.5418$ Å) with a resolution of 0.02° of 2θ from 10° to 80°. The morphologies of the as-synthesized products were characterized by field emission scanning electron microscope (FE-SEM; Hitachi, S-4800) at an acceleration voltage of 10.0 kV. The element composition was characterized by a Horiba EX250 X-ray energy-dispersive spectrometer (EDX) associated with the FESEM. Transmission electron microscopy (TEM) images and the corresponding selected area electron diffraction (SAED) patterns were captured on the JEOL 2100F high resolution transmission electron microscope at an acceleration voltage of 200 kV (JEOL, Japan). The X-ray photoelectron spectroscopy (XPS) analysis was conducted on a Multilab 2000 XPS system with a monochromatic Mg K α source and a charge neutralizer; the binding energies were referenced to the C 1s peak at 284.4 eV of the surface adventitious carbon. Ultraviolet-visible diffuse reflectance (UV-Vis DR) spectra of the samples were measured from the optical absorption spectra using a UV-Vis spectrophotometer (UV-2550 PC, Shimadzu). Fine BaSO₄ powder is used as a standard for baseline and the spectra are recorded in a range 200-800 nm. The Brunauer–Emmett–Teller (BET) specific surface area (S_{BET}) of the powders was analysed by nitrogen adsorption in a Micromeritics ASAP 2020 nitrogen adsorption apparatus (USA). All the as-prepared samples were degassed at 180 °C prior to nitrogen adsorption measurements. The BET surface area was determined by a multipoint BET method using the adsorption data in the relative pressure (P/P_0) range of 0.05–0.3. A desorption isotherm was used to determine the pore size distribution via the Barret–Joyner–Halender (BJH) method, assuming a cylindrical pore model.

Hydrogen evolution measurements: Photocatalytic reactions for hydrogen evolution were carried out in a closed gas circulation system with an external-irradiation Pyrex cell, which was placed about 10 cm under a 300 W xenon lamp (PLS SXE300, Beijing Trusttech Co. Ltd., China) with an average light intensity of 5 mW cm⁻². The diameter of the reactor is ca. 63 mm almost equal to the facula size of the light source. To compare the photocatalytic activities for H₂ production of

the as-obtained F-Ta₂O₅ and naked Ta₂O₅ HNs and C-Ta₂O₅ particles, 20 mg of the samples without co-catalysts were dispersed in 100 mL of aqueous solution containing 20% methanol in volume. The amount of evolved gas was determined by a thermal conductivity detector (TCD) gas chromatograph (TECHCOMP, 7890Ⅲ), which was connected to the system with a circulating line. At the same time, the overall water-splitting experiment was also conducted under the same condition but the methanol aqueous solution is replaced by pure water.

Supplementary information images

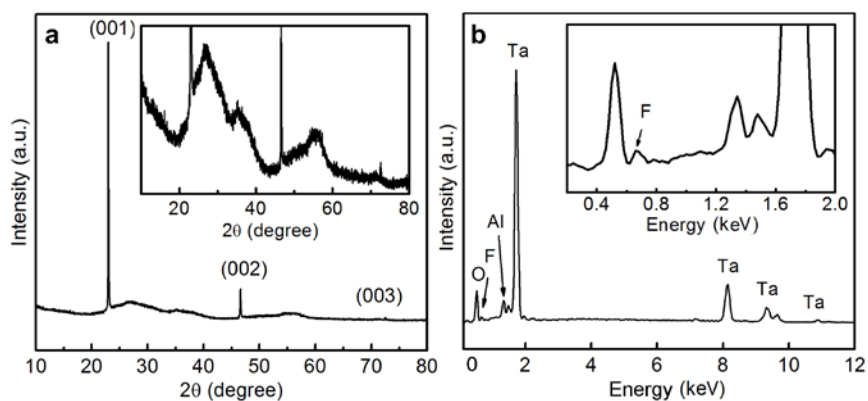


Fig. S1 (a) XRD pattern and (b) EDX spectrum of the typical samples of F-Ta₂O₅. The inset in (a) shows the enlarged pattern; the inset in (b) shows magnification spectrum from 0.2 to 2 keV.

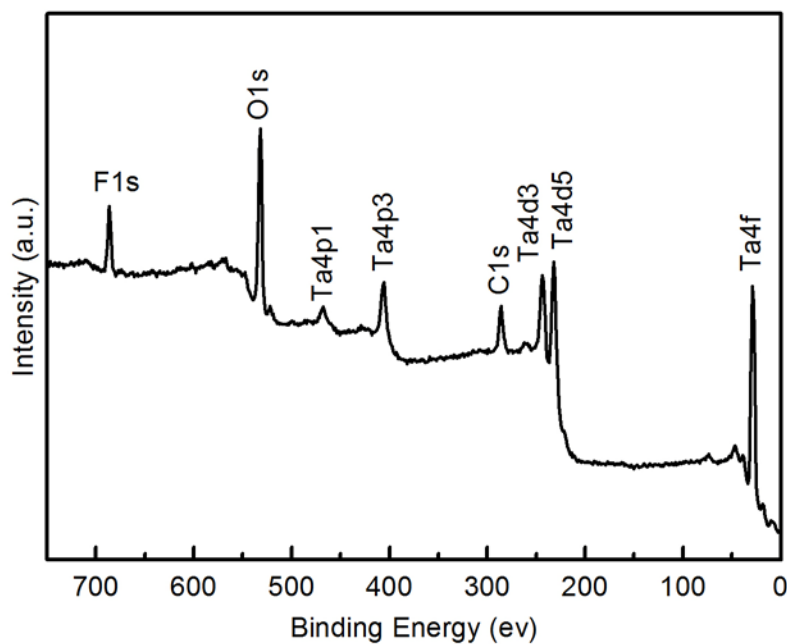


Fig. S2 XPS spectrum of the F-Ta₂O₅ samples.

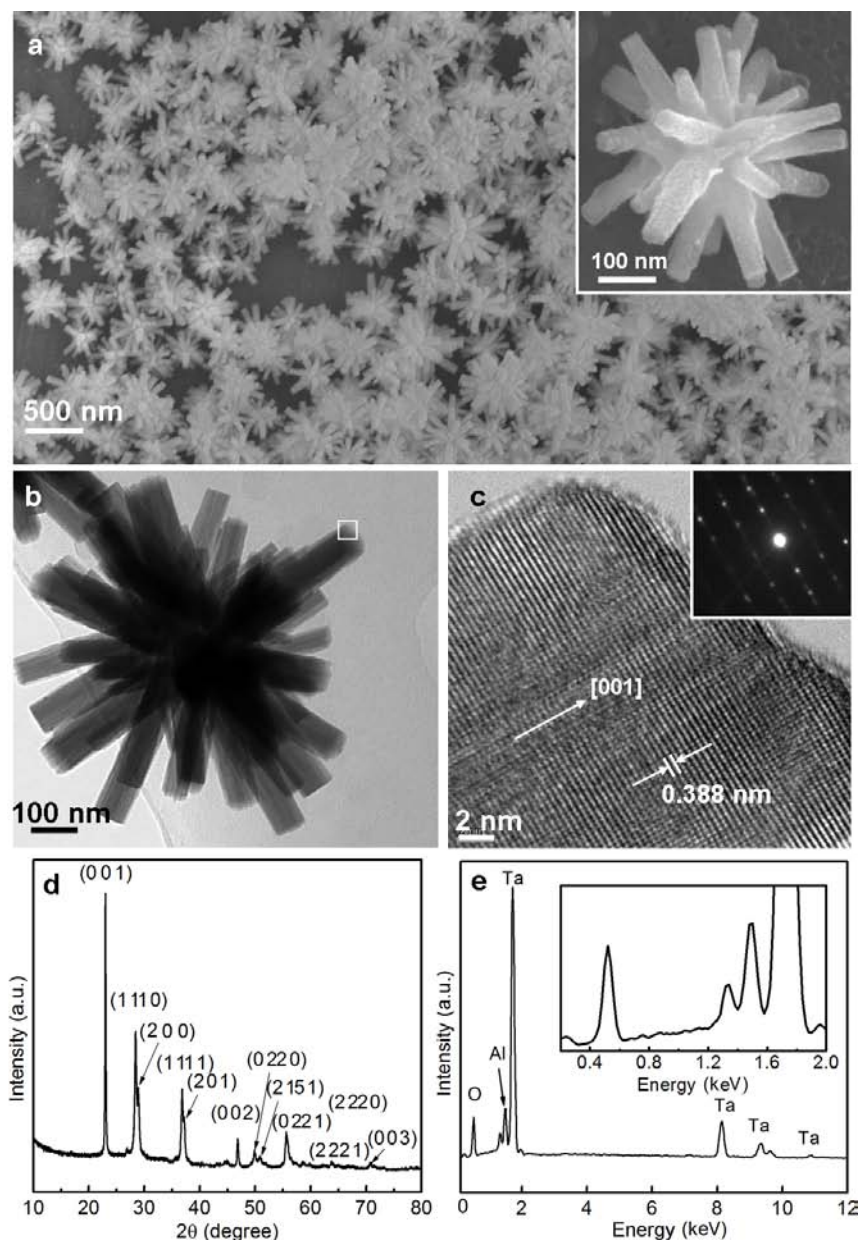


Fig. S3 (a) SEM images of Ta₂O₅ HNs; (b) TEM image of a single Ta₂O₅ HN; (c) HRTEM image of a single Ta₂O₅ nanorod indicated by a rectangular frame in (b); (d) XRD pattern and (e) EDX spectrum of the obtained samples of Ta₂O₅. The inset in (a) shows the high magnification SEM image of a single Ta₂O₅ HN; the inset in (c) shows the corresponding SAED pattern of the single Ta₂O₅ nanorod; the inset in (e) shows the magnified spectrum from 0.2 to 2 keV.

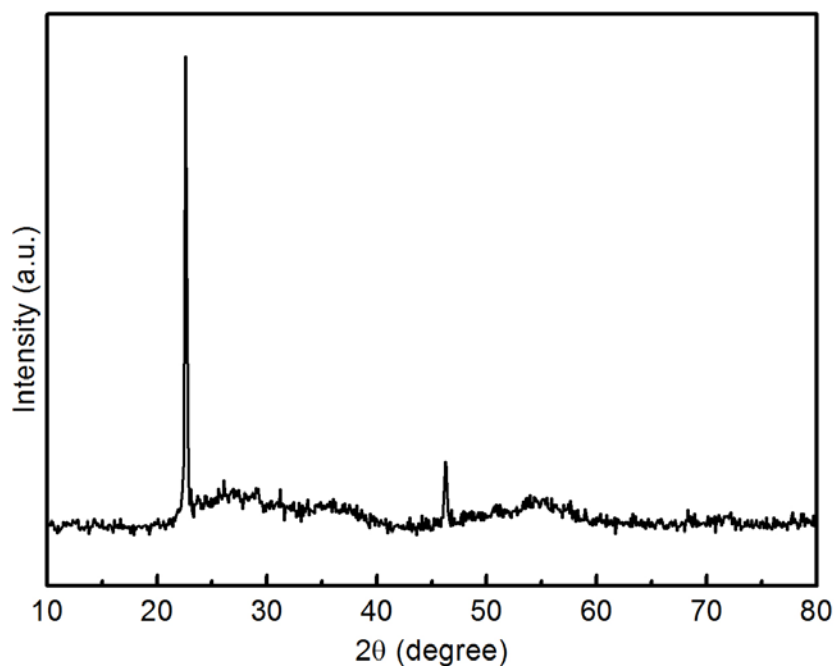


Fig. S4 XRD pattern of the white-colour samples obtained at t of 2 h

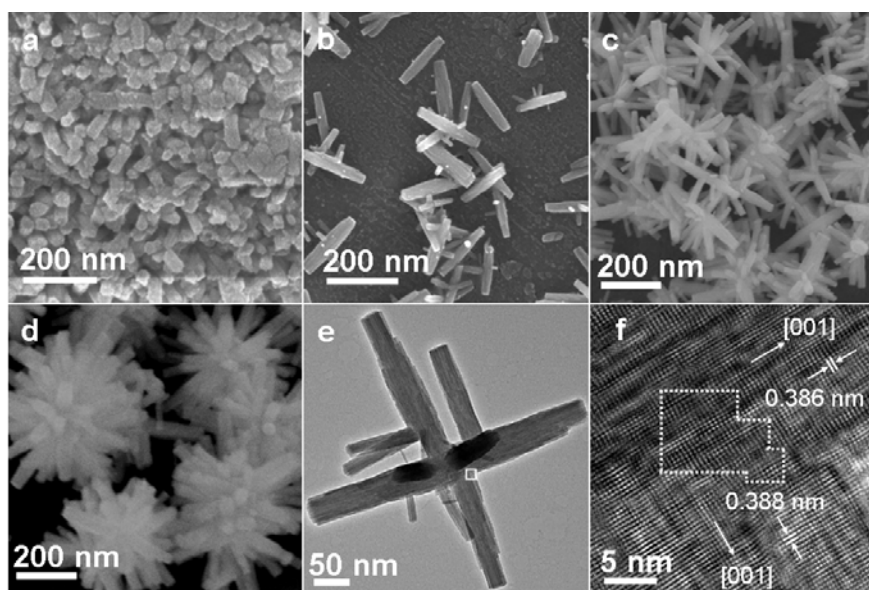


Fig. S5 SEM images of the F-Ta₂O₅ samples obtained at different t of (a) 2, (b) 4, (c) 6 and (d) 8 h; (e) TEM and (f) HRTEM images of the F-Ta₂O₅ samples obtained at 6 h.

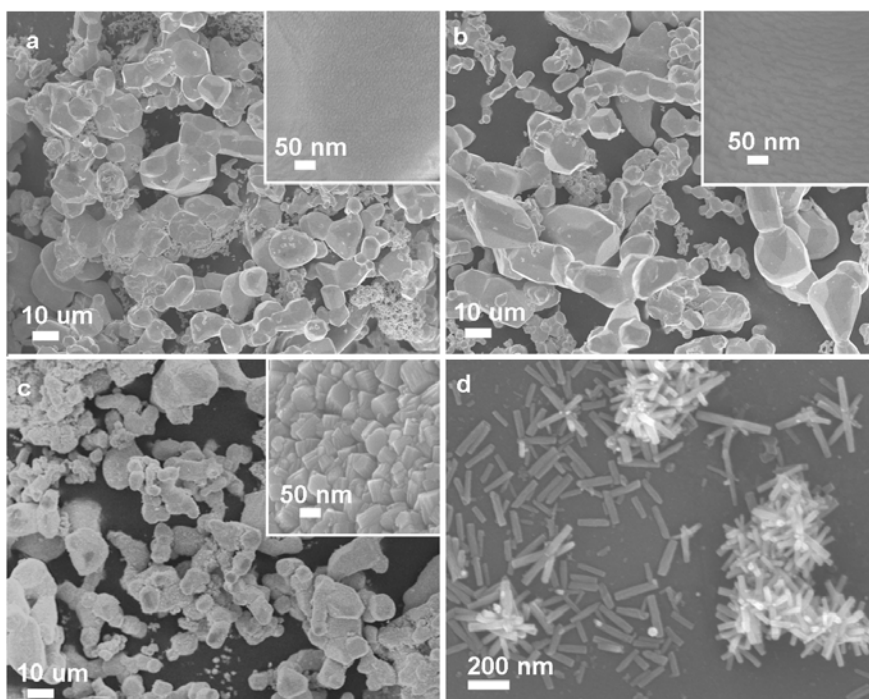


Fig. S6 SEM images of (a) the raw Ta powders and the samples obtained after a hydrothermal process in the absence of (b) HF and H₂O₂, (c) HF, or (d) H₂O₂. All the insets show the high magnification SEM images of the surface of the corresponding single particles.

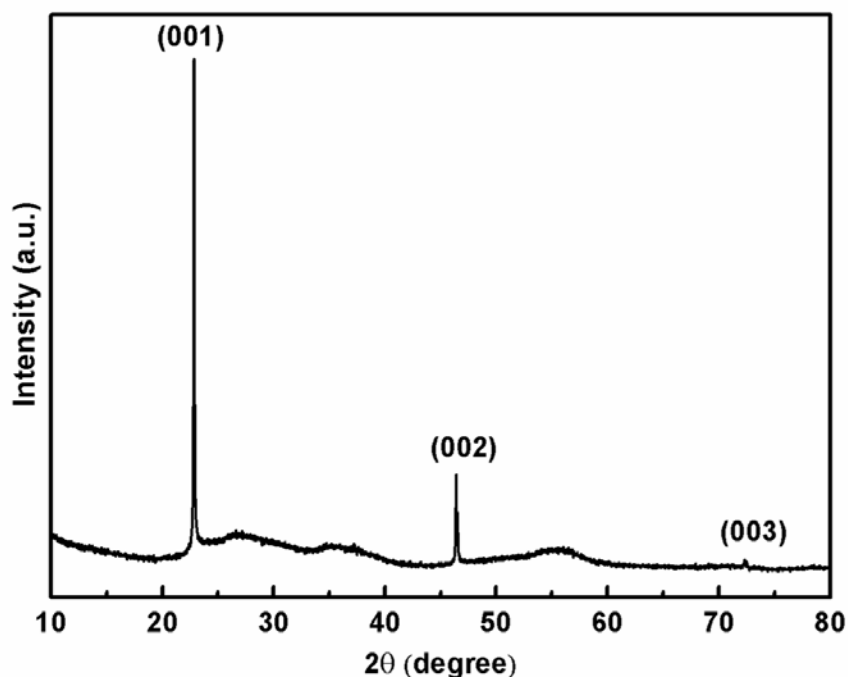


Fig. S7 XRD pattern of the samples obtained in the absence of H₂O₂.

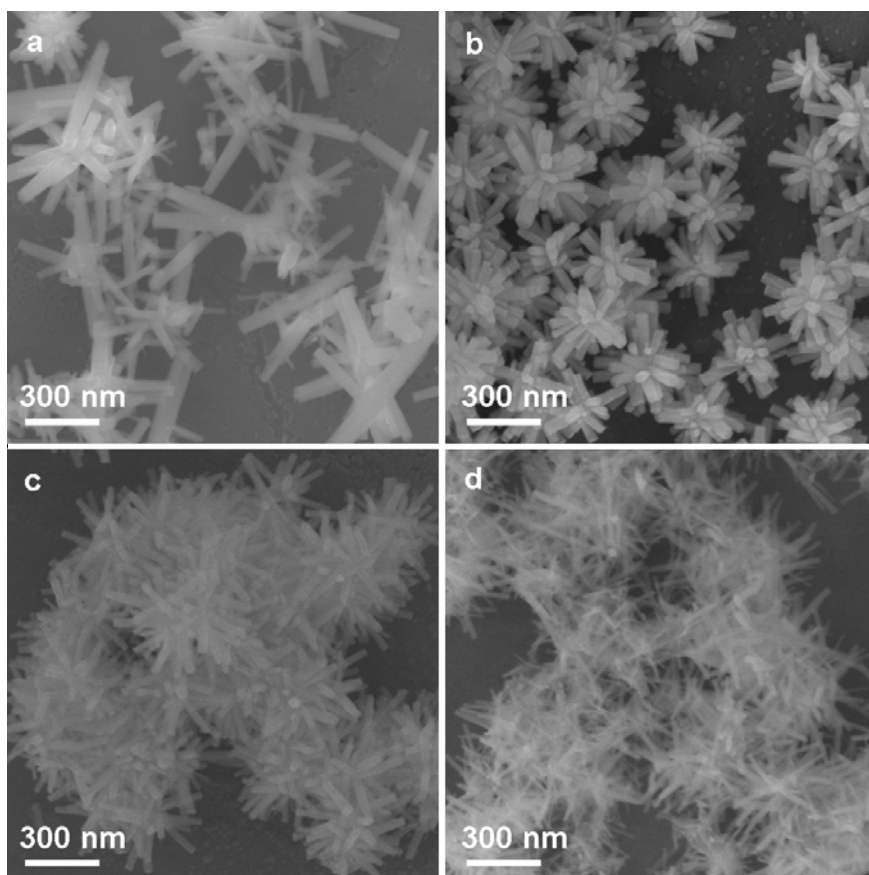


Fig. S8 SEM images of the F-Ta₂O₅ samples obtained at different [HF] of (a) 0.100 M, (b) 0.133 M, (c) 0.167 M, and (d) 0.200 M.

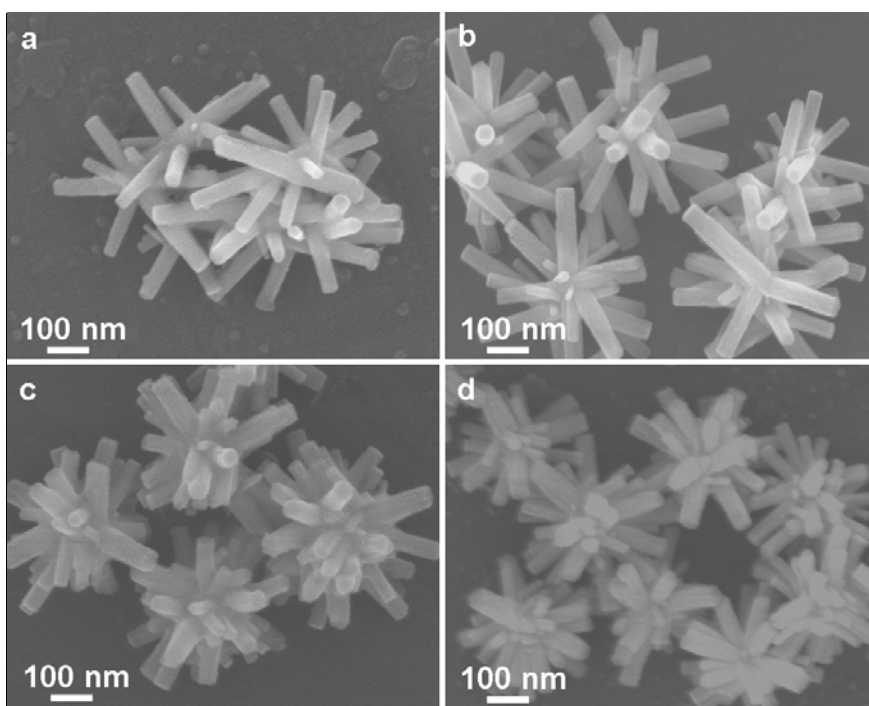


Fig. S9 SEM images of the F-Ta₂O₅ samples obtained at different [H₂O₂] of (a) 3.0 M, (b) 4.0 M, (c) 5.0 M, and (d) 6.0 M

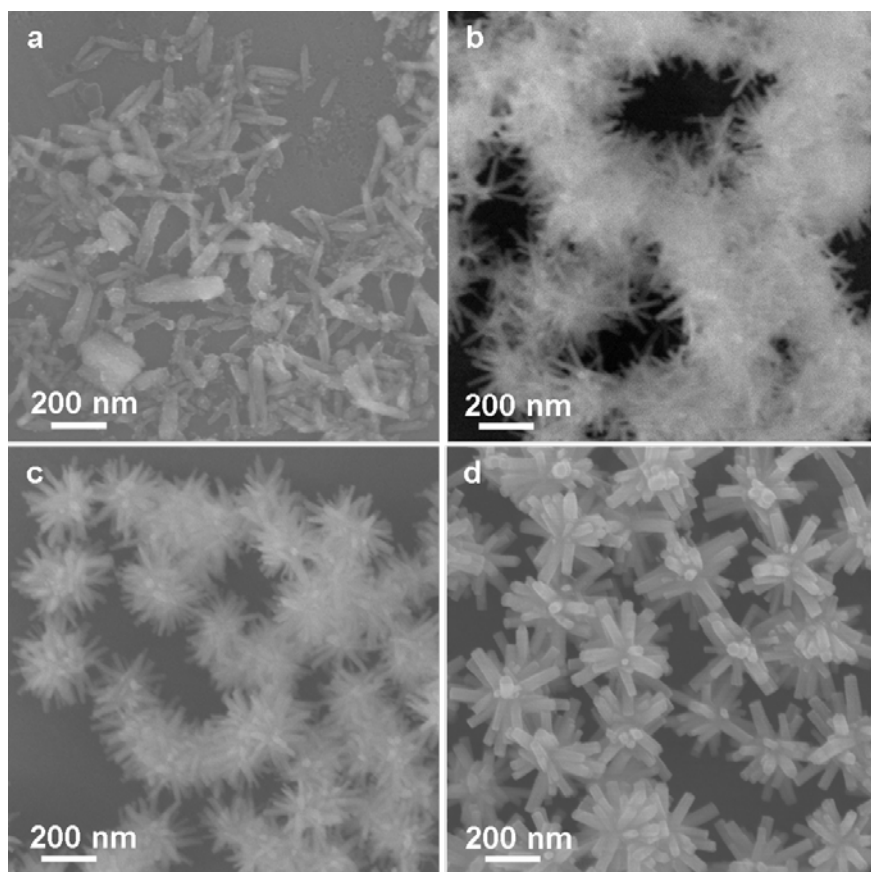


Fig. S10 SEM images of the F-Ta₂O₅ samples obtained at different hydrothermal temperatures of (a) 180 °C, (b) 200 °C, (c) 220 °C, and (d) 240 °C

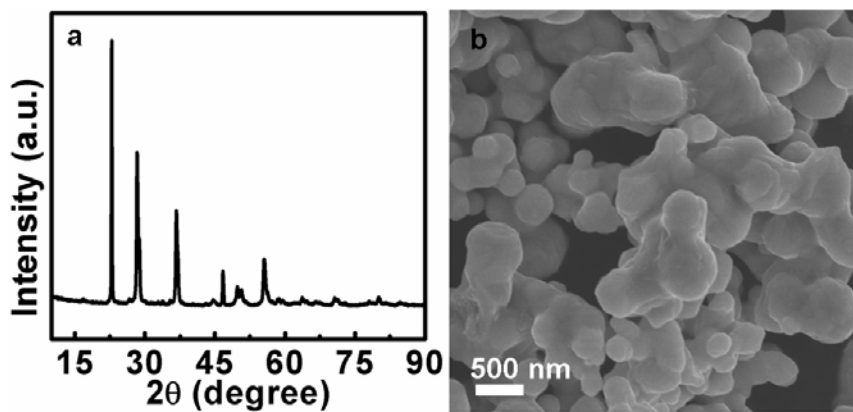


Fig. S11 (a) XRD pattern and (b) SEM images of the C-Ta₂O₅ particles

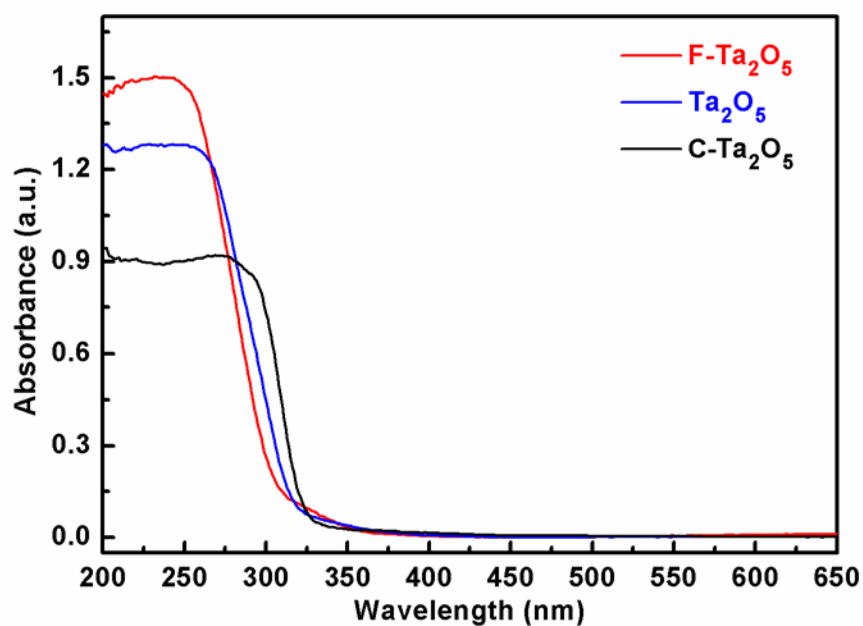


Fig. S12 UV-Vis absorption spectra of F-Ta₂O₅, Ta₂O₅ and C-Ta₂O₅ samples.

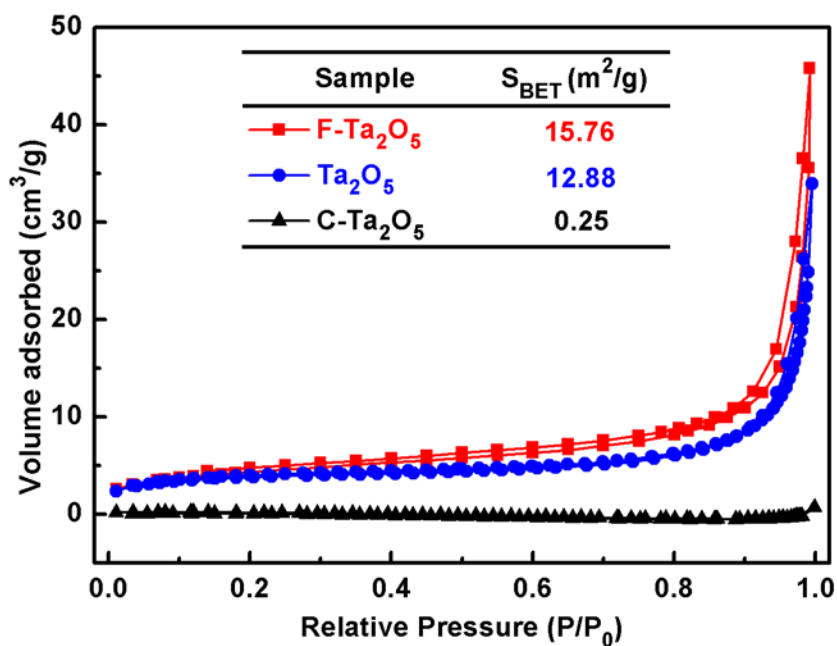


Fig. S13 Nitrogen adsorption–desorption isotherms and the corresponding S_{BET} of F-Ta₂O₅, Ta₂O₅ and C-Ta₂O₅ samples.

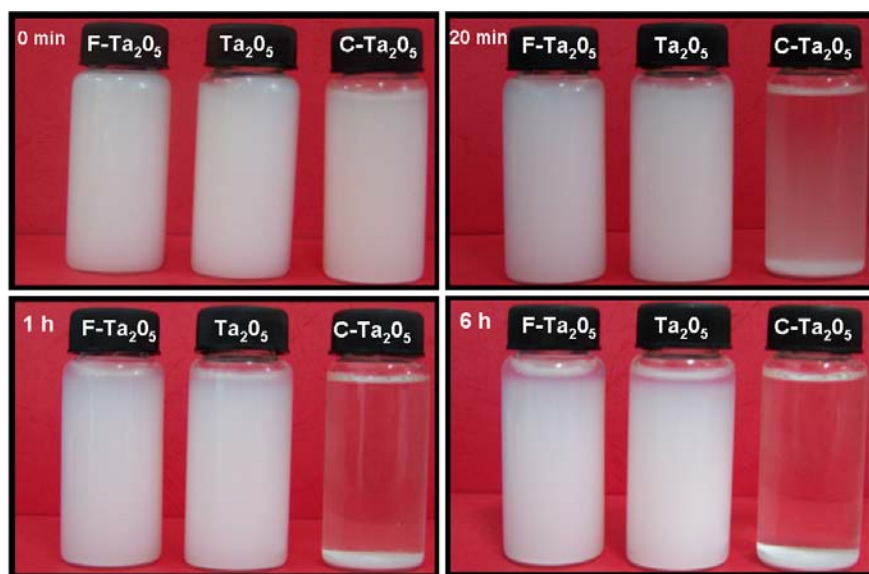


Fig. S14 The pictures of the aqueous suspensions containing F-Ta₂O₅, Ta₂O₅ or C-Ta₂O₅ samples after standing different times.

Graphical Abstract

Novel hierarchical nanostructures of F-Ta₂O₅ and Ta₂O₅ hyperbranched single crystalline nanorods, which exhibit much more excellent photocatalytic activities for H₂ production from water than commercial Ta₂O₅ particles (C-Ta₂O₅), have successfully been prepared *via* an organic additive-free hydrothermal method.

